Pergamon

Control Eng. Practice, Vol. 4, No. 2, pp. 167-178, 1996

0967-0661/96 $15.00 + 0.00

PII:S0967-0661(95)00223-5

CONSTRUCTIVE EMPIRICAL MODELLING OF LONGITUDINAL VEHICLE DYNAMICS USING LOCAL MODEL NETWORKS

K.J. Hunt*, J.C. Kalkkuhl*, H. Fritz and T.A. Johansen*****

**Daimler-Benz Research and Technology, Alt-Moabit 96A, D-10559 Berlin, Germany (hunt@DBresearch-berlin.de)*
***Daimler-Benz Research and Technology, D-70546 Stuttgart, Germany*
****SINTEF Automatic Control, N-7034 Trondheim, Norway*

(Received August 1995; in final form December 1995)

Abstract. In this paper a number of empirically derived parametric models of longitudinal vehicle dynamics are compared. The vehicle concerned is a fully instrumented Mercedes-Benz commercial lorry. The main focus is on a class of models known as local model networks. In this structure, a number of simple local linear models are combined ('interpolated') by 'scheduling' on a number of physical variables which are known to, or can be found to, capture the system non-linearities. Following extensive experimentation involving the use of constructive search for operating regime decomposition, it is concluded that scheduling on gear and throttle angle leads to the best overall model. Local 1st-order linear ARX models are found to be sufficient. For comparison, a non-linear model of Hammerstein type and a multi-layer perceptron neural-network are also identified.

Keywords. Automotive control, Non-linear models, Dynamic modelling, System identification

1. INTRODUCTION

In the very near future, 'intelligent' cruise control systems will be introduced to the automotive market. These systems will include sensors which can measure the distance to the vehicle in front. Using the distance measurement, an appropriate setpoint for the vehicle speed can be autonomously selected. The end goal is to automatically maintain a safe inter-vehicle spacing. This functionality has to work over the full range of vehicle speed.

Standard cruise control systems typically operate at speeds above 40 km/h, and commonly utilise a fixed PID-type algorithm. The problem in automotive speed control lies mainly in the widely varying non-linear dynamic behaviour of the vehicle. The more stringent requirements of intelligent cruise control demand a non-linear control approach (Fritz, 1995).

This paper presents the results of experiments on non-linear modelling of longitudinal vehicle dynamics. The models are ultimately used for intelligent cruise control design and verification, but these control aspects are reported elsewhere. The experiments used data gathered from an experimental vehicle, a Mercedes-Benz commercial lorry.

The non-linear models employed are known as local model networks (Johansen and Foss, 1992). They are based on the smooth combination (interpolation) of a set of locally valid linear models. The local model network has a transparent structure which allows a direct analysis of local model properties (e.g. stability). The local model network can also be directly used as the basis of non-linear control design, resulting in an interpolating network of local controllers (Żbikowski *et al.*, 1994).

As a first step, global linear models of throttle–speed dynamics are identified. Second, a model comprising one linear model for each gear is identified. The overall model is formed using the measured gear to switch between each linear model. The idea of using vehicle speed to schedule local models is then investigated. It is concluded that this brings no significant improvement. Following this, constructive search algorithms for operating regime decomposition are employed. The result is that scheduling on gear and throttle angle leads to the best overall model.

It is concluded that the constructive approach to non-linear empirical modelling with local model networks has significant advantages over traditional neural-network modelling of non-linear dynamics. A black-box neural-network is developed to facilitate the comparison (Hunt *et al.*, 1992). A non-linear model of Hammerstein type (static non-linearity followed by linear transfer-function) is also identified for comparative purposes.

2. NON-LINEAR VEHICLE DYNAMICS

A simplified realistic dynamic longitudinal model of the vehicle is developed which contains the essential effects and non-linearities (Fritz, 1995). The model mainly describes the powertrain system. It includes the combustion engine, automatic transmission and rear axle differential. The automatic transmission consists of a torque converter and a 4-speed automatic gearbox. Figure 1 shows these components and their dependencies. The double-framed blocks indicate non-linear input-output relations.

The model of the complete powertrain consists mainly of two ordinary differential equations, which are coupled by two characteristic functions of the torque converter.

The actuator systems for throttle and brake are described by additional state equations. The first equation of motion describes the dynamic behaviour of the engine. The state variable is the engine angular velocity ω_e. The second state equation describes the longitudinal motion of the vehicle. For this, a simplified one-wheel model with only one driving wheel is developed. It is assumed that the vehicle is equipped with an antilock braking system. Tyre slip is not taken into account. Consequently, the vehicle speed v can be determined as the product of wheel angular velocity ω and wheel radius r. The non-linear behaviour of the engine is described by operating curves which give the engine torque T_e as a function of throttle angle α and the engine angular velocity:

$$T_e = f_e(\alpha, \omega_e). \tag{1}$$

The torque converter is a fluid coupling device used in the automatic transmission for its damping and torque multiplication characteristics. The torque at the input side (pump) is transferred to the output side (turbine) as a result of oil-induced flow from the pump. The pump is directly attached to the engine and therefore rotates at the engine angular velocity ($\omega_p = \omega_e$). With the ratio ξ between the angular velocity of turbine and pump ($\xi = \omega_t/\omega_p$), the functional dependencies of the turbine and the pump torques are given by

$$T_p = f_1(\xi, \omega_e^2), \tag{2}$$

$$\mu = T_t/T_p = f_2(\xi), \tag{3}$$

where μ is the torque gain from torque converter input to torque converter output. Given current values for the state variables ω_e and ω, the unknown turbine torque can be determined from the two non-linear characteristic torque converter functions.

The behaviour of the automatic transmission system can also be described with non-linear characteristic functions. The change of gear is a function of the throttle position α, the velocity v or the angular velocity ω and the gear $g(t)$ at the current time t. The algorithm to determine the gear can be expressed in discrete form by the function

$$g(t+1) = f_g(\alpha(t), v(t), g(t)). \tag{4}$$

For each gear there exists a characteristic reference speed function for shifting to the next higher gear, and another characteristic reference speed function for shifting to the next lower gear depending on the throttle α. With these characteristic gearshift functions it is possible to determine the predicted gear and the gear ratio i_g of the automatic transmission. With the rear axle gear ratio i_d the angular velocity of the turbine is given by:

$$\omega_t = i_d i_g \omega. \tag{5}$$

The vehicle is equipped with two electronically controlled actuator systems, one for throttle and one for the brake. The throttle is modelled by a 1st-order lag system

$$\tau_\alpha \dot{\alpha}(t) + \alpha(t) = u_\alpha(t - d_\alpha) \tag{6}$$

with the delay time d_α, the input u_α, and the time constant τ_α. The model of the electronically controlled brake system consists of a 1st-order lag expression and a time delay component

$$\tau_p \dot{p}(t) + p(t) = u_p(t - d_p) \tag{7}$$

where p is the brake pressure, u_p is the input, τ_p is the time constant and d_p is the delay time. The brake torque is defined to be proportional to the brake pressure

$$T_b(t) = k_p p(t) \tag{8}$$

where k_p is the proportionality constant. The longitudinal motion of the vehicle is influenced by several disturbances which are summarized by an external disturbing torque

$$T_{ex} = T_w + T_r + T_c. \tag{9}$$

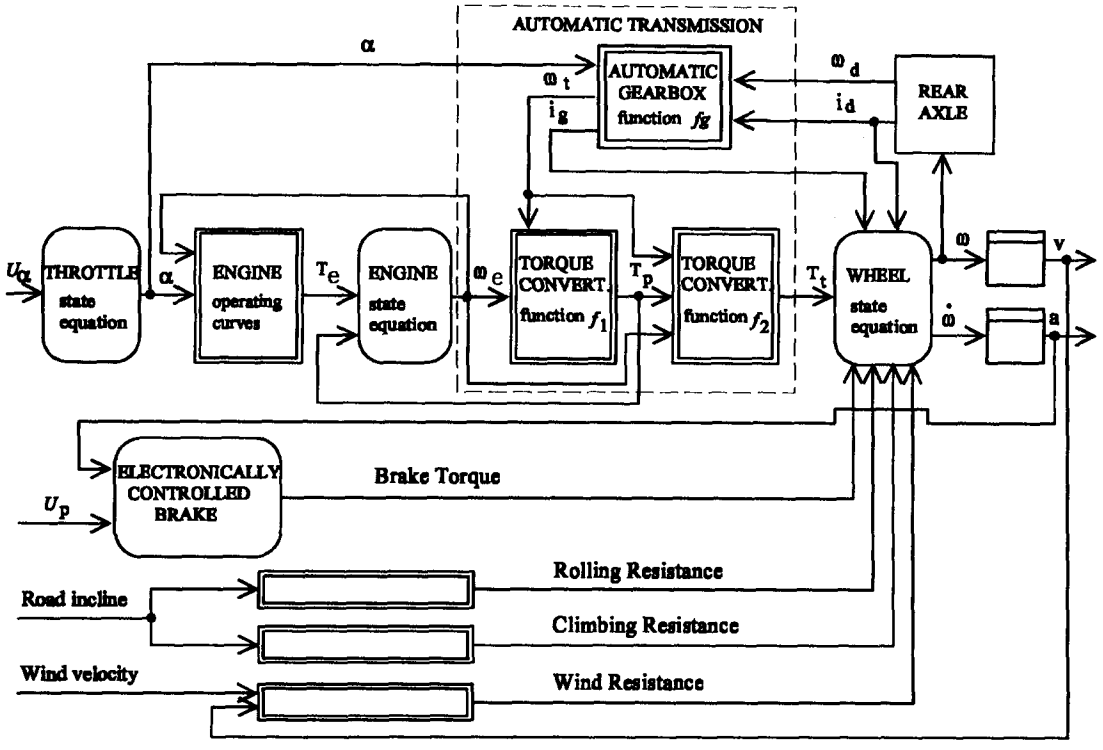

Fig. 1. Powertrain components

The aerodynamic resistance is given by

$$T_w = c_a(v - v_w)^2 r \tag{10}$$

with the aerodynamic drag coefficient c_a and the wind velocity v_w. The rolling resistance is

$$T_r = k_r mg\cos(\alpha_i)r \tag{11}$$

where k_r is the coefficient of rolling resistance, m the vehicle mass, g the gravitational acceleration and α_i the road incline angle. The climb torque is given by

$$T_c = mg\sin(\alpha_i)r. \tag{12}$$

With this preliminary work the two main state equations can be given. The equation of motion for the engine is

$$\dot{\omega}_e = \frac{T_e - T_p}{J_e} \tag{13}$$

where J_e is the inertia of the engine. The longitudinal motion of the vehicle can be described by the state equation

$$\dot{\omega} = \frac{T_t i_g i_d \eta_g \eta_d - T_b - T_{ex}}{J_g i_d^2 \eta_d + J_d + 4J + mr^2} \tag{14}$$

where η_g and η_d are the efficiency coefficients of the automatic transmission and the rear axle differential respectively. J_g, J_d, and J are the inertias of transmission, rear axle differential and wheel respectively.

The automatic transmission of the truck is equipped with a converter lockup clutch. Therefore the model described above is only valid for low speeds. If the speed of the vehicle exceeds a certain limit the converter lockup clutch is closed. Because of the resulting rigid connection between the wheel and the engine ($\omega_e = i_d i_g \omega$), the model can be simplified. This results in only one state equation. In this case the longitudinal motion of the vehicle is given by the state equation

$$\dot{\omega} = \frac{T_e i_g i_d \eta_g \eta_d - T_b - T_{ex}}{J_e i_g^2 i_d^2 \eta_g^2 \eta_d^2 + J_g i_d^2 \eta_d + J_d + 4J + mr^2}. \tag{15}$$

The aim in this paper will be to empirically determine the relationship between throttle angle α and speed v.

3. LINEAR MODELLING

In this section standard linear identification approaches for longitudinal dynamics modelling are considered. This will provide an important insight into the underlying dynamic properties of the system; it will also establish a benchmark for evalu-

ation of the non-linear methods which are investigated in the sequel.

3.1 *Model structure*

The overall non-linear relationship between throttle and speed can be approximately described in the discrete-time functional form

$$v(t) = f(v(t-1)\ldots v(t-nv);\ldots \\ \ldots\alpha(t-k)\ldots\alpha(t-k-n\alpha)) + e(t), \tag{16}$$

which is known as an NARX model representation. The vehicle speed at time instant t depends on past values of speed and throttle angle according to the non-linear function f. Notice that f need not be smooth since gear switching can be seen as a discontinuous phenomenon. The integers nv and $n\alpha$ determine the order of the system and k is an integer input-output time delay, which depends on the plant dead-time and the sampling period. Here, $e(t)$ represents the effects of unmodelled behaviour.

The system (16) can be linearised for a fixed gear and small deviations around some equilibrium point (v^*, α^*). Considering only 1st-order terms in a Taylor expansion of f, this results in the transfer-function

$$\tilde{v}(t) = \frac{q^{-k}B(q^{-1})}{A(q^{-1})}\tilde{\alpha}(t) + \frac{1}{A(q^{-1})}e(t). \tag{17}$$

Here, $\tilde{v}$ and $\tilde{\alpha}$ represent deviations from the equilibrium:

$$\tilde{v}(t) = v(t) - v^*, \tag{18}$$

$$\tilde{\alpha}(t) = \alpha(t) - \alpha^*. \tag{19}$$

In (17), A and B are polynomials in the delay operator[1] q^{-1}:

$$A(q^{-1}) = 1 + a_1q^{-1} + \ldots + a_{nv}q^{-nv}, \tag{20}$$

$$B(q^{-1}) = b_0 + b_1q^{-1} + \ldots + b_{n\alpha}q^{-n\alpha}. \tag{21}$$

The coefficients a_i, b_i correspond to the elements of the Jacobian (i.e. the partial derivatives) of the non-linear function f in the Taylor expansion around (v^*, α^*).

The linear model (17) can be expressed in terms of v and α by substituting from (18)–(19),

$$v(t) = \frac{q^{-k}B(q^{-1})}{A(q^{-1})}\alpha(t) + \frac{d}{A(1)} + \frac{1}{A(q^{-1})}e(t). \tag{22}$$

[1] For any signal $x(t)$, $q^{-1}x(t) = x(t-1)$.

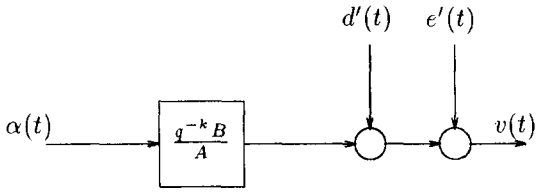

Fig. 2. Linear model

In the above equation, d is an equilibrium-dependent offset term defined by

$$d = A(1)v^* - B(1)\alpha^*. \tag{23}$$

This linear model structure is depicted in Figure 2. In the figure, the quantities d' and e' are related to d and e in (22) through $d' = d/A(1)$ and $e'(t) = e(t)/A(q^{-1})$.

Extensive modelling experiments have been carried out using the model structure (22). These experiments have shown that a model of 1st or 2nd order is sufficient to capture the main dynamics. A 2nd-order model is obtained by selecting $nv = 2$ and $n\alpha = 1$. For a 1st-order model $nv = 1$ and $n\alpha = 0$. The identified models are used for the design of closed-loop speed controllers. Taking account of the desired closed-loop bandwidth, it has been found reasonable to select a sampling time of 0.48s. With this choice of sampling period, the appropriate value of k is $k = 1$ (the total plant dead-time is less than one sample period). These choices for the structure parameters lead to the 1st-order model

$$v(t) = \frac{b_0q^{-1}}{1 + a_1q^{-1}}\alpha(t) + \frac{d}{1 + a_1} + \ldots \\ \ldots + \frac{1}{1 + a_1q^{-1}}e(t), \tag{24}$$

or the 2nd-order model

$$v(t) = \frac{q^{-1}(b_0 + b_1q^{-1})}{1 + a_1q^{-1} + a_2q^{-2}}\alpha(t) + \frac{d}{1 + a_1 + a_2} \\ \ldots + \frac{1}{1 + a_1q^{-1} + a_2q^{-2}}e(t). \tag{25}$$

3.2 *Parameter estimation*

This section describes the algorithms used to estimate the local model parameters. The model (22) can be explicitly expressed in terms of $v(t)$,

$$v(t) = -A'(q^{-1})v(t) + q^{-k}B(q^{-1})\alpha(t) + \ldots \\ \ldots + d + e(t), \tag{26}$$

with $A'(q^{-1}) = A(q^{-1}) - 1$. Note that the right-hand-side of this equation depends only on past values of the output, $v(t-1)\ldots$. Assuming there

is no information on the term $e(t)$, the best prediction of the system output based on data up to the point $t-1$ is given by

$$\hat{v}(t) = -A'(q^{-1})v(t) + q^{-k}B(q^{-1})\alpha(t) + d. \tag{27}$$

Parameter-estimation algorithms deal most conveniently with dynamic models expressed in regression format. The form of equation (27) allows this to be achieved very simply as

$$\hat{v}(t) = \theta^T \phi(t-1), \tag{28}$$

where the *parameter vector* θ is defined as

$$\theta^T = (a_1, a_2, \ldots a_{nv}; b_0, b_1, \ldots b_{n\alpha}; d), \tag{29}$$

and the *regression vector* ϕ is

$$\begin{aligned}\phi^T(t-1) = (&-v(t-1), \ldots -v(t-nv); \ldots \\ &\ldots \alpha(t-k), \ldots \alpha(t-k-n\alpha); 1).\end{aligned} \tag{30}$$

Note that the parameter vector contains all unknown parameters of the model (22), i.e. the coefficients of the polynomials A and B, and the offset term d.

The objective of parameter estimation is to determine the best estimate of the parameter vector, denoted $\hat{\theta}$, based on N measured observations of the system inputs $\alpha(t)$ and $g(t)$, and the output $v(t)$; $t = 1 \ldots N$. A measure of model fidelity is provided by the least-squares criterion

$$\begin{aligned}J_N(\theta) &= \frac{1}{N}\sum_{t=1}^{N} w(t)(v(t) - \hat{v}(t))^2 = \\ &= \frac{1}{N}\sum_{t=1}^{N} w(t)(v(t) - \theta^T\phi(t-1))^2,\end{aligned} \tag{31}$$

where $w(t)$ is a data weighting term. This criterion is minimised with respect to θ:

$$\begin{aligned}\hat{\theta} = &\left(\sum_{t=1}^{N} w(t)\phi(t-1)\phi^T(t-1)\right)^{-1} \\ &\sum_{t=1}^{N} w(t)\phi(t-1)v(t).\end{aligned} \tag{32}$$

This is the solution used in the experiments reported in Section 3.3. Full details of this approach to parameter estimation can be found in a number of textbooks on system identification, e.g. (Ljung and Söderström, 1983; Ljung, 1987).

For the 1st- and 2nd-order models (24)–(25), the respective parameter and regression vector pairs are

$$\theta^T = (a_1, b_0, d), \tag{33}$$

$$\phi^T(t-1) = (-v(t-1), \alpha(t-1), 1) \tag{34}$$

and

$$\theta^T = (a_1, a_2, b_0, b_1, d), \tag{35}$$

$$\begin{aligned}\phi^T(t-1) = (&-v(t-1), -v(t-2), \ldots \\ &\ldots \alpha(t-1), \alpha(t-2), 1).\end{aligned} \tag{36}$$

3.3 *Experimental results*

Experiments were carried out using a Mercedes-Benz experimental lorry. The vehicle was instrumented to provide measurements of the necessary variables: throttle angle (%/100), speed (m/s) and gear (1–4). A wide variety of input signals was applied over the full operational range. The resulting data were split into an estimation set and a validation set. The ratio of estimation to validation data was 60/40. The two data sets are shown respectively in Figures 3 and 4. The data were gathered on a mainly flat road, thereby ensuring that road incline disturbances do not feature in the identification. Inclusion of the gear measurement is important as it is known *a priori* that the vehicle dynamics change abruptly as the gear changes. This opens the possibility of constructing models consisting of sub-models, with each sub-model being associated with a particular gear. This idea is pursued below and in later sections.

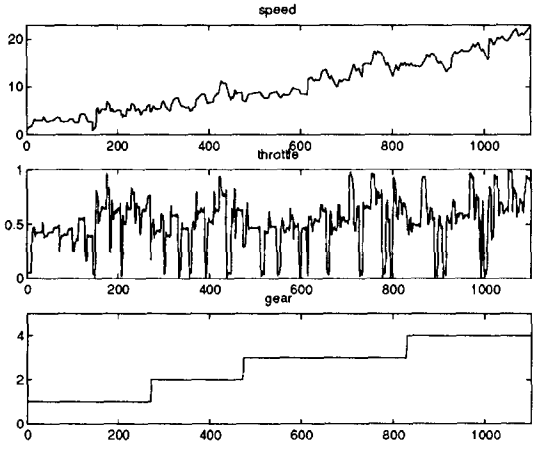

Fig. 3. Estimation data

Global linear model. As a first step a global linear model structure was investigated; a single linear model is used for all gears. Table 1 shows the parameters of a 1st (M1) and 2nd order (M2) model, together with a measure of model fit, the root-mean-square residuals RES $= \sqrt{J_N(\hat{\theta})}$.

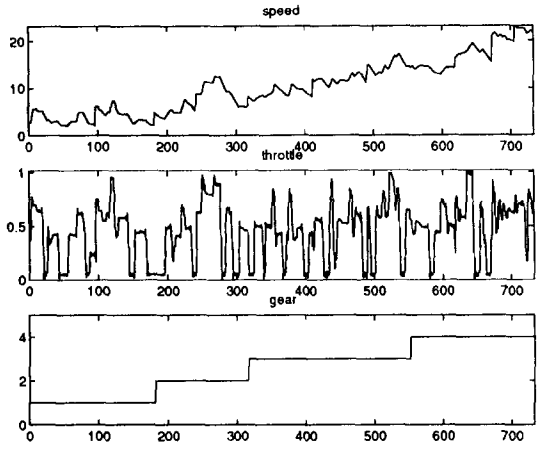

Fig. 4. Validation data

Table 1. Global linear models M1 and M2: 1st- and 2nd-order

Gear	Transfer-function	Offset d	RES
1–4	$\frac{0.5974q^{-1}}{1-0.9907\,q^{-1}}$	−0.1981	0.1440
1–4	$\frac{q^{-1}(0.7986-0.5844q^{-1})}{1-1.6\,q^{-1}+0.6037\,q^{-2}}$	−0.0660	0.1033

One linear model for each gear. The next model structure consisted in estimating one linear model for each gear. The current gear is directly used to switch between models. The estimated parameters with 1st-order models (M3) are shown in Table 2, and those for 2nd-order models (M4) in Table 3. Inspection of Table 3 shows that in the model for 4th gear one pole is very close to the origin, and suggests that this model is in reality 1st-order. The 1st-order model for 4th gear is therefore kept. The results are shown in Table 4 (M5).

Table 2. Linear models M3: one for each gear (1st-order)

Gear	Transfer-function	Offset d	RES
1	$\frac{1.278q^{-1}}{1-0.8439\,q^{-1}}$	0.0066	0.1211
2	$\frac{0.8477q^{-1}}{1-0.9546\,q^{-1}}$	−0.0663	
3	$\frac{0.665q^{-1}}{1-0.9768\,q^{-1}}$	−0.0599	
4	$\frac{0.5778q^{-1}}{1-0.9803\,q^{-1}}$	0.0181	

Comparison and validation of linear models. In order to validate and compare models M1–M5, the root-mean-square prediction error (APE) for a ballistic simulation and the root-mean-square 1-step-ahead prediction error (1SA) were computed for each model using the validation data set. The results are set out in Table 11. (M4 is now omitted as the results of all validation tests were very similar for M4 and M5.)

Table 3. Linear models M4: one for each gear (2nd-order)

Gear	Transfer-function	Offset d	RES
1	$\frac{q^{-1}(1.322-0.8411\,q^{-1})}{1-1.562\,q^{-1}+0.6248\,q^{-2}}$	0.0151	0.0853
2	$\frac{q^{-1}(0.8925-0.6359\,q^{-1})}{1-1.687\,q^{-1}+0.7049\,q^{-2}}$	0.0091	
3	$\frac{q^{-1}(0.6915-0.4577\,q^{-1})}{1-1.631\,q^{-1}+0.6397\,q^{-2}}$	−0.0094	
4	$\frac{q^{-1}(0.528+0.0613\,q^{-1})}{1-0.955\,q^{-1}+0.0233\,q^{-2}}$	0.0385	

Table 4. Linear models M5: one for each gear (1st/2nd-order)

Gear	Transfer-function	Offset d	RES
1	$\frac{q^{-1}(1.322-0.8411\,q^{-1})}{1-1.562\,q^{-1}+0.6248\,q^{-2}}$	0.0151	0.0854
2	$\frac{q^{-1}(0.8925-0.6359\,q^{-1})}{1-1.687\,q^{-1}+0.7049\,q^{-2}}$	0.0091	
3	$\frac{q^{-1}(0.6915-0.4577\,q^{-1})}{1-1.631\,q^{-1}+0.6397\,q^{-2}}$	−0.0094	
4	$\frac{0.5778q^{-1}}{1-0.9803\,q^{-1}}$	0.0357	

The conclusions are that switching local models according to gear brings a very significant improvement in the overall model. Increasing the local model order to 2 greatly improves the average residual on the estimation data, but does not consistently lead to an improvement on the validation data. It can be concluded that overfitting is occurring with 2nd-order local models, and that 1st-order local models are most appropriate. Thus, model M3 is the best to date.

Figure 5 shows a plot of the simulated output of model M1 (the simplest model) together with the measured output for the validation data set. The corresponding plot for model M3 is shown in Figure 6. In these, and in the following simulations, the dotted line is the model output and the solid line is the measured vehicle speed.

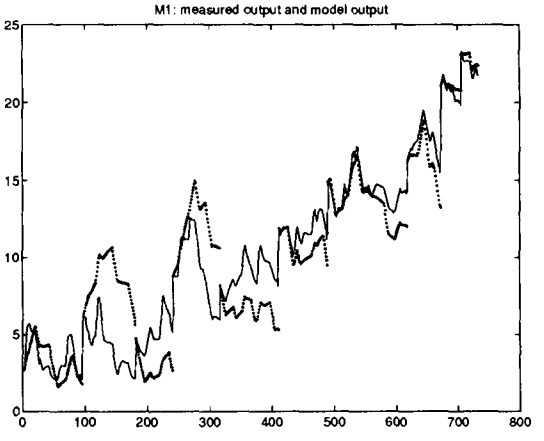

Fig. 5. Simulation of M1 on validation data

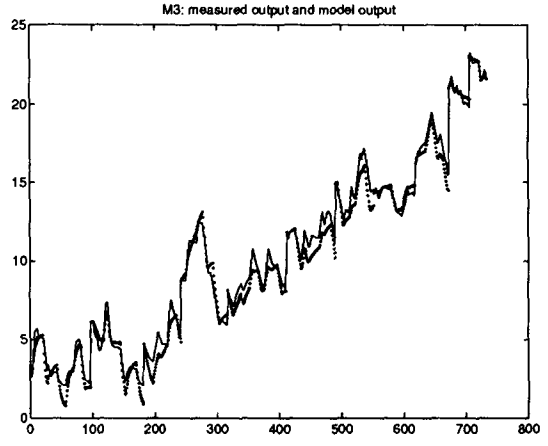

Fig. 6. Simulation of M3 on validation data

4. LOCAL MODEL NETWORK

The linear model (22) is valid for a fixed gear in the region of a single equilibrium point. The local model network is a structure which is valid for multiple equilibria (Johansen and Foss, 1992).

4.1 *Model structure*

First, for each gear a number M of equilibria are chosen, and a locally valid linear model is obtained for each of them. The i-th equilibrium is denoted by (v_i^*, α_i^*), and the locally valid linearisation at this point is

$$v(t) = \frac{q^{-k}B_i(q^{-1})}{A_i(q^{-1})}\alpha(t) + \frac{d_i}{A_i(1)} + \ldots + \frac{1}{A_i(q^{-1})}e(t). \quad (37)$$

The problem now is to combine the local models in some way in order to produce a model which is globally valid as the system operating point changes. To do this, a set of validity functions is introduced. The validity function ρ_i for each local model provides a measure of how close the current operating point of the system (as defined by the speed $v(t-1)$) is to the corresponding equilibrium v_i^*. When v is close to v_i^* the validity $\rho_i(v(t-1))$ is close to one, and far from v_i^* it is close to zero. The validity functions are constrained to satisfy

$$\sum_{i=1}^{M} \rho_i(v) = 1 \quad (38)$$

for all v. The output of each local one-step-ahead predictor is defined by

$$\hat{v}_i(t) = \theta_i^T \phi(t-1). \quad (39)$$

The M parameter vectors θ_i contain the local A_i, B_i and d_i parameters as in (29). The regression vector ϕ is global (i.e. is used by all local models) and has the form (30). The overall local model network one-step-ahead predictor is formed from the weighted sum of the local model one-step-ahead predictors, where the weighting is done using the validity functions,

$$\hat{v}(t) = \hat{v}_1(t)\rho_1(v(t-1)) + \ldots + \hat{v}_M(t)\rho_M(v(t-1)) = \sum_{i=1}^{M} \hat{v}_i(t)\rho_i(v(t-1)). \quad (40)$$

With local linear models (39) the local model network one-step-ahead predictor takes the form

$$\hat{v}(t) = \phi^T(t-1)\sum_{i=1}^{M} \theta_i \rho_i(v(t-1)). \quad (41)$$

4.2 *Parameter estimation*

One way to do the local model parameter estimation is to perform identification experiments in restricted regions around the equilibria. The local parameters can then be estimated using the procedures given in Section 3.2. Alternatively, a set of local parameter estimators can be employed. In this case, the local criteria are defined by

$$J_{N,i}(\theta_i) = \frac{1}{N}\sum_{t=1}^{N} \rho_i(v(t-1))(v(t) - \hat{v}_i(t))^2 = \frac{1}{N}\sum_{t=1}^{N} \rho_i(v(t-1))(v(t) - \theta_i^T\phi(t-1))^2, \quad (42)$$

Here, the weighting term is $w(t) = \rho_i(\phi(t-1))$ such that the data is effectively smoothly partitioned into M sets. The regression vector corresponds to (30). The local parameter estimates are (c.f. (32))

$$\hat{\theta}_i = \left(\sum_{t=1}^{N} \rho_i(v(t-1))\phi(t-1)\phi^T(t-1)\right)^{-1} \sum_{t=1}^{N} \rho_i(v(t-1))\phi(t-1)v(t). \quad (43)$$

The third alternative is to estimate all local model parameters simultaneously using a global criterion (31) with $\theta^T = (\theta_1^T, \ldots, \theta_M^T)$ and the predictor (40). Estimating the parameters on the basis of a global criterion or several local criteria lead to local models with qualitatively different properties. With local criteria, the aim is to find local models that are close to local linearizations of the system, while with a global criterion the aim is to find local models that when interpolated give a global model that is close to the system. Hence,

with a global criterion, it may not be possible to interpret the local models separately. On the other hand, the global model will typically give better predictions when it is identified with a global criterion, as long as the model structure is parsimonious. Further details on the relationship between local and global estimation criteria can be found in (Murray-Smith and Johansen, 1995).

4.3 *Experimental results*

In this section the measured gear is again used to switch between four individual models. In this case, however, the individual models are local model networks as described above. For each gear two operating points were chosen: one for lower speeds for that gear, and one for higher speeds. The operating-point speeds chosen correspond to the centres of the validity functions used in the interpolation of the local models. The resulting models, together with the root-mean-square residuals (RES) on the estimation data, are shown in Table 5. The results presented are for 1st-order local models. A structure having 2nd-order local models was able to significantly reduce the RES on the estimation data set, but for the validation set the quantitative validation measures used were worse. The offset terms d_i were also estimated but are omitted from the table. Note that these results are for local learning.

Table 5. M6: linear models scheduled on gear and speed

Gear	Low speed	High speed	RES
1	$\frac{1.202q^{-1}}{1-0.8232\,q^{-1}}$	$\frac{1.378q^{-1}}{1-0.8456\,q^{-1}}$	0.1193
2	$\frac{0.976q^{-1}}{1-0.9659\,q^{-1}}$	$\frac{0.8091q^{-1}}{1-0.9486\,q^{-1}}$	
3	$\frac{0.6267q^{-1}}{1-0.9749\,q^{-1}}$	$\frac{0.6826q^{-1}}{1-0.9758\,q^{-1}}$	
4	$\frac{0.5211q^{-1}}{1-0.9856\,q^{-1}}$	$\frac{0.6142q^{-1}}{1-0.9769\,q^{-1}}$	

The average prediction error (APE) and one-step-ahead prediction error (1SA) for this model on the validation set are given in Table 11.

Variation of the local model poles over the operating regimes is depicted in Figure 7. This figure also gives a good impression of the operating regime decomposition, with hard switching according to gear and smooth interpolation with speed. Consideration of the results presented in Table 5 and Figure 7 shows that for each gear the variation in local model parameters is very small. In comparison with M3 (no speed scheduling, see Table 2), the average residual on the estimation data is slightly improved, but the average- and one-step-ahead prediction errors on the validation

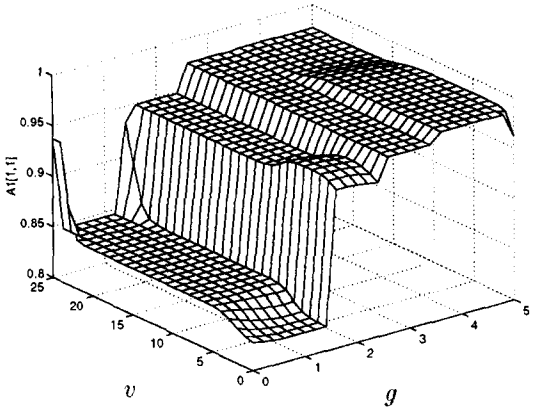

Fig. 7. M6: variation of system pole over operating regimes

data are worse. Thus, it is not beneficial to schedule using speed, and model M3 remains the best to date.

5. CONSTRUCTIVE GENERATION OF THE LMN

5.1 *Model structure and parameter estimation*

The local model network formulation in this section is slightly more general in the sense that the local operating points are not restricted to physical equilibria. For a fixed gear, M operating points ϕ_i^* are defined using

$$\phi_i^* = (v_{i,1}^* \ldots v_{i,nv}^*; \alpha_{i,1}^* \ldots \alpha_{i,n\alpha+1}^*, 1)^T \quad (44)$$

where $i = 1 \ldots M$.[2] Linearisation of (16) around ϕ_i^* leads also to the model structure (37), i.e. the one-step-ahead predictor

$$\hat{v}(t) = (1 - A_i(q^{-1}))v(t) + q^{-k}B_i(q^{-1})\alpha(t) + \ldots \\ \ldots + d_i. \quad (45)$$

In this instance, however, the definition of d_i is (c.f. (23))

$$d_i = v_i^* + \sum_{j=1}^{nv} a_{ij} v_{i,j}^* - \sum_{j=0}^{n\alpha} b_{ij} \alpha_{i,j+1}^*, \quad (46)$$

where $v_i^* = f(\phi_i^*)$.

The information vector ϕ now defines the operating point of the system and in general this vector must be used to determine the validity of the local models. Thus, the local model network one-step-ahead predictor now has the form (c.f. (40))

$$\hat{v}(t) = \sum_{i=1}^{M} \hat{v}_i(t)\rho_i(\phi(t-1))$$

[2] When ϕ_i^* does correspond to an equilibrium then $v_{i,1}^* = v_{i,2}^* = \ldots = v_i^*$ and $\alpha_{i,1}^* = \alpha_{i,2}^* = \ldots = \alpha_i^*$.

with local models according to (39),

$$\hat{v}_i(t) = \theta_i^T \phi(t-1).$$

For a 1st-order model the operating point vector is $\phi(t-1) = (v(t-1), \alpha(t-1), 1)^T$, and the local model network one-step-ahead predictor simplifies to

$$\hat{v}(t) = \sum_{i=1}^{M} \hat{v}_i(t)\rho_i(v(t-1), \alpha(t-1)), \quad (47)$$

where the '1' from ϕ is not used as it has no effect on the scheduling. To allow a simple geometrical interpretation of the local model structure, a 1st-order LMN of this form is used in the remainder of this section. Experimentation has shown that increasing the order of the model to 2 produces no appreciable improvement.

With the linearly parameterized one-step-ahead predictor (47) the parameter estimation problem can be solved using the least-squares methods outlined in the previous sections.

5.2 *Experimental results*

In this section a heuristic search algorithm (Johansen and Foss, 1995*a*; Johansen and Foss, 1995*b*) is applied to search for the best decomposition of the operating range into operating regimes, according to α and v. This algorithm compares a wide range of promising decompositions using a statistical criterion computed by means of the estimation data.

Interactive use of the constructive algorithm resulted in an LMN with 7 local models as shown in Table 6 (global estimation criterion) and Table 7 (local estimation criteria). The d_i-parameters were also identified, but they are omitted from the tables. For the first to third gears, the LMN has different local models for low and high throttle, while for the fourth gear such a refinement did not give a significant improvement.

The constructive algorithm had the opportunity to decompose on the basis of both throttle and speed, but it is observed that only the throttle was actually applied for decomposition. Hence, the main non-linearities are captured by throttle and gear. This also explains and confirms the modest improvements in Section 4 where the operating range was decomposed *a priori* on the basis of speed and gear.

The difference between local and global estimation criteria can be seen by comparing M7a and M7b. With a global estimation criterion, an LMN results which is a global model with the best prediction performance, but with local models that may be significantly different from local linearization, because the global estimation takes advantage of interaction effects between them. Local estimation criteria, on the other hand, give a biased LMN with slightly poorer prediction performance, but with local models that can consistently be interpreted as local linearizations of the system.

Table 6. M7a: Linear models scheduled on gear and throttle, identified with a global estimation criterion

Gear	Low throttle	High throttle	RES
1	$\frac{0.285q^{-1}}{1-0.863q^{-1}}$	$\frac{2.267q^{-1}}{1-0.717q^{-1}}$	0.0917
2	$\frac{0.472q^{-1}}{1-0.953q^{-1}}$	$\frac{1.680q^{-1}}{1-0.817q^{-1}}$	
3	$\frac{0.235q^{-1}}{1-0.965q^{-1}}$	$\frac{0.338q^{-1}}{1-0.933q^{-1}}$	
4	$\frac{0.578q^{-1}}{1-0.980q^{-1}}$		

Table 7. M7b. Linear models scheduled on gear and throttle, identified with local estimation criteria

Gear	Low throttle	High throttle	RES
1	$\frac{0.620q^{-1}}{1-0.864q^{-1}}$	$\frac{2.516q^{-1}}{1-0.745q^{-1}}$	0.0981
2	$\frac{0.702q^{-1}}{1-0.964q^{-1}}$	$\frac{2.191q^{-1}}{1-0.853q^{-1}}$	
3	$\frac{0.487q^{-1}}{1-0.974q^{-1}}$	$\frac{1.038q^{-1}}{1-0.954q^{-1}}$	
4	$\frac{0.578q^{-1}}{1-0.980q^{-1}}$		

A finer partitioning into operating regimes using three local linear models corresponding to low, medium and high throttle for each gear was also tried. The model M8 identified using a global identification criterion is shown in Table 8. Again, the d_i parameters were identified but are omitted from the table.

The root-mean-square prediction error (APE) and the root-mean-square one-step-ahead prediction error (1SA) for models M7a, M7b and M8 are given in Table 11. Clearly, there is a very significant quantitative improvement when compared to

Table 8. M8: Linear models scheduled on gear and throttle, RES = 0.0861

Gear	Low throttle	Medium throttle	High throttle
1	$\frac{0.094q^{-1}}{1-0.870q^{-1}}$	$\frac{2.363q^{-1}}{1-0.741q^{-1}}$	$\frac{2.564q^{-1}}{1-0.747q^{-1}}$
2	$\frac{0.358q^{-1}}{1-0.973q^{-1}}$	$\frac{2.615q^{-1}}{1-0.863q^{-1}}$	$\frac{2.721q^{-1}}{1-0.853q^{-1}}$
3	$\frac{0.308q^{-1}}{1-0.979q^{-1}}$	$\frac{2.006q^{-1}}{1-0.936q^{-1}}$	$\frac{0.635q^{-1}}{1-0.959q^{-1}}$
4		$\frac{0.578q^{-1}}{1-0.980q^{-1}}$	

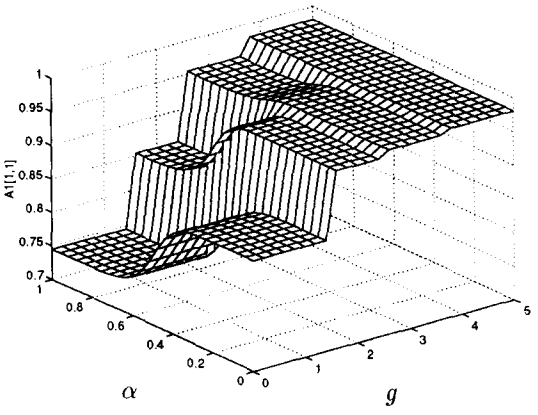

Fig. 8. M7b: variation of system pole over operating regimes

models M1–M6, none of which used throttle for scheduling.

Variation of the local model poles over the operating regimes is depicted in Figure 8.

Figure 9 shows a plot of the simulated output of M7b, together with the measured output for the validation data set.

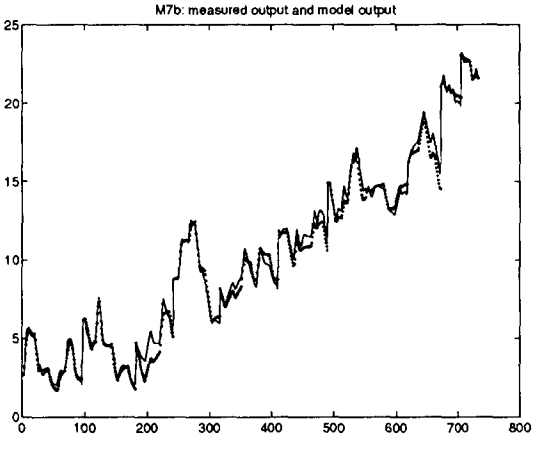

Fig. 9. Simulation of M7b on validation data

6. HAMMERSTEIN MODEL

The results obtained so far show a strong dependence of the model parameters on the throttle angle. This fact suggests a simple 1st-order Hammerstein structure,

$$v(t) = av(t-1) + \beta(\alpha(t-1)) \qquad (48)$$

where the static input non-linearity β is given in parameterised form as

$$\beta(\alpha) = \sum_{k=1}^{n} \theta_k \rho_k(\alpha). \qquad (49)$$

Two different spline approximation schemes were used to estimate the input non-linearity $\beta(\alpha)$ for each gear:

M9: linear splines with 6 discretisation points
M10: cubic splines with 4 discretisation points

Tables 9–10 show the estimated a-values (the poles) and the average residuals for the estimation data.

Table 9. M9: Hammerstein model using linear splines (a parameters)

Gear	a	RES
1	0.8034	0.0917
2	0.9047	
3	0.9559	
4	0.9719	

Table 10. M10: Hammerstein model using cubic splines (a parameters)

Gear	a	RES
1	0.8034	0.0922
2	0.9043	
3	0.9558	
4	0.9719	

In Figure 10 the approximation results for the input non-linearities are depicted with linear interpolation shown as a dashed line and cubic interpolation shown as a solid line. The Hammerstein hypothesis was checked by plotting the values $v(t)-av(t-1)$ against the input values $\alpha(t-1)$ for the data samples.

The simulated output of model M9, together with the measured output for the validation data set, is shown in Figure 11. For model M9 and M10 the validation measures APE and 1SA are given in Table 11.

7. NEURAL-NETWORK MODEL

A number of black-box neural-network structures were applied to the modelling task. The type of neural-network employed was a multilayer perceptron (MLP), and the training method was back-propagation. The network was supplied with three inputs: speed, throttle and gear at time $t-1$. This leads to the following input-output structure

$$v(t) = f_{nn}(v(t-1), \alpha(t-1), g(t-1)). \qquad (50)$$

Following extensive testing and validation, a model having a single hidden layer with five

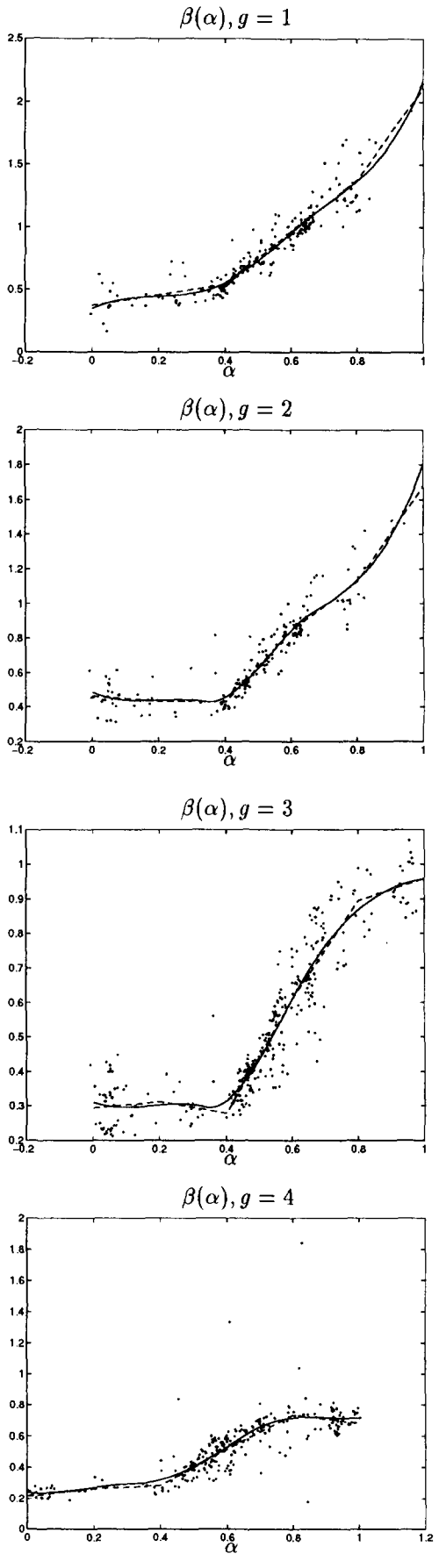

Fig. 10. Estimated input nonlinearities

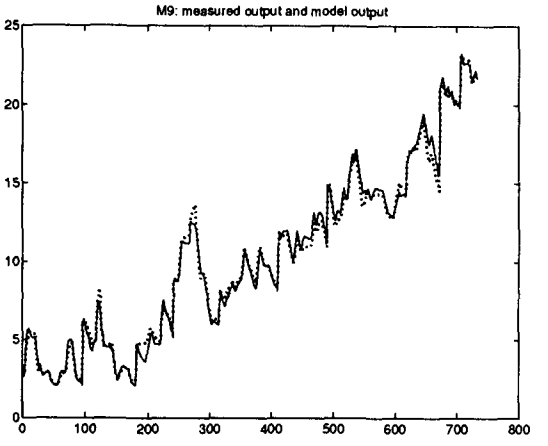

Fig. 11. Simulation of M9 on validation data

non-linear processing units was selected. For this model, which is labelled M11, the average residual on the training data was 0.0809. The one-step-ahead prediction error and average prediction error on the validation data are listed in table 11.

8. VALIDATION AND COMPARISON OF MODELS

The validation measures for each of the models are collected together in Table 11. The best models are the local model networks scheduled on gear and throttle, and the Hammerstein models switched according to gear and with a static throttle-input non-linearity. The three best models, M7a, M8 and M10, have similar average prediction errors, but the one-step-ahead performance of M7a and M8 is significantly better.

By considering Table 8, conclusions regarding the qualitative changes in the system with respect to operating point can be drawn. As gear changes from 1 to 4, the system pole moves consistently towards the unit circle and the dynamic response is therefore slower. Within gears 1–3, the low-throttle region is characterised by slower poles and low gain. In the middle region the pole becomes significantly faster and the gain higher. In 1st and 2nd gears the poles and gains remain similar for the high-throttle region, while in 3rd gear the system becomes slower with a lower gain. These results corresponds to physical intuition since the vehicle is in general most responsive in a mid-range throttle position, while displaying a less responsive, saturation-like, behaviour at low and high throttle positions. The identified input non-linearities for the Hammerstein models further confirm these findings.

Table 11. Comparison of model validation results

Model	Description	APE	1SA
M1	1st-order linear	2.389	0.1643
M2	2nd-order linear	2.113	0.1352
M3	1 model/gear (1st-order)	0.6392	0.1471
M5	1 model/gear (1st/2nd-order)	0.6672	0.1298
M6	gear/speed scheduled	0.7076	0.1477
M7a	gear/throttle scheduled	0.4158	0.1122
M7b	gear/throttle scheduled	0.4755	0.1141
M8	gear/throttle scheduled	0.3652	0.1094
M9	Hammerstein (linear splines)	0.4099	0.1560
M10	Hammerstein (cubic splines)	0.4115	0.1550
M11	MLP	0.5252	0.1181

9. CONCLUSIONS

The following conclusions can be drawn from the results:

- Local dynamics are dominantly 1st-order. Using 2nd- or higher-order local linear models leads to overfitting.
- The vehicle dynamics depend strongly on gear and throttle angle.
- There is no benefit in using vehicle speed to schedule local linear models.

A local model network with switching according to gear, and smooth interpolation with throttle angle, was found to be the best model structure. The employment of constructive search algorithms was instrumental in deriving this model structure. An important advantage of the LMN structure is that the local models can be directly interpreted and their dynamic properties fully analysed. The local models can furthermore be used as the basis of a set of local feedback controller designs. The models in Sections 3–5 were obtained with the MATLAB-based tool ORBIT[3] (Johansen, 1995).

A Hammerstein model gives results comparable to the simplest gear-throttle-scheduled local model network. By introducing additional local models, however, the performance of the LMN was further improved. The multilayer perceptron neural-network gives reasonable results, but direct interpretation of the resulting model in terms of poles and time-constants is not possible. Moreover, the model does not lend itself directly to control design. General aspects of control design with empirically-derived non-linear models are discussed in (Kalkkuhl and Hunt, 1996).

[3] ORBIT stands for Operating Regime Based modeling and Identification Tool.

10. REFERENCES

Fritz, H. (1995). Neural speed control for autonomous road vehicles. In: *Proc. 2nd IFAC Conference on Intelligent Autonomous Vehicles, Helsinki, Finland.* pp. 285–290.

Hunt, K. J., D. Sbarbaro, R. Żbikowski and P. J. Gawthrop (1992). Neural networks for control systems: a survey. *Automatica* **28**(6), 1083–1112.

Johansen, T. A. (1995). ORBIT - User's guide and reference. Technical Report STF48-A95013. SINTEF, Trondheim, Norway.

Johansen, T. A. and B. A. Foss (1992). A NARMAX model representation for adaptive control based on local models. *Modelling, Identification and Control* **13**(1), 25–39.

Johansen, T. A. and B. A. Foss (1995*a*). Identification of non-linear system structure and parameters using regime decomposition. *Automatica* **31**, 321–326.

Johansen, T. A. and B. A. Foss (1995*b*). Semi-empirical modeling of non-linear dynamic systems through identification of operating regimes and local models. In: *Neural Network Engineering in Dynamic Control Systems* (K. Hunt, G. Irwin and K. Warwick, Eds.). pp. 105–126. Springer-Verlag, London.

Kalkkuhl, J. C. and K. J. Hunt (1996). Discrete-time neural model structures for continuous-time non-linear systems. In: *Neural Adaptive Control Technology I* (R. Żbikowski and K. J. Hunt, Eds.). World Scientific Publishing.

Ljung, L. (1987). *System Identification — Theory for the User.* Prentice-Hall. Englewood Cliffs, New Jersey, USA.

Ljung, L. and T. Söderström (1983). *Theory and Practice of Recursive Identification.* MIT Press. London.

Murray-Smith, R. and T. A. Johansen (1995). Local learning in local model networks. In: *4th IEE Intern. Conf. on Artificial Neural Networks.* pp. p40–46.

Żbikowski, R., K. J. Hunt, A. Dzieliński, R. Murray-Smith and P. J. Gawthrop (1994). A review of advances in neural adaptive control systems. *Int. J. Neural Systems.* Submitted for publication.